NUMERICAL SIMULATION OF FATIGUE DELAMINATION GROWTH UNDER MODE I LOADING CONDITIONS

Piotr Bajurko, Kamila Czajkowska

Institute of Aviation
Krakowska Av. 110/114 ,02-256 Warsaw, Poland
tel.: +48 22 8460805, fax:+ 48 22 8462912
e-mail:piotr.bajurko@ilot.edu.pl, kamila.czajkowska@ilot.edu.pl

Piotr Czarnocki

Institute of Aeronautics and Applied Mechanics, Warsaw University of Technology
Nowowiejska Street 24, 00-665 Warsaw, Poland
tel.: +48 22 2345856, fax:+48 22 628 2587
e-mail: pecz@meil.pw.edu.pl

Daniel Szeląg

Institute of Aviation
Krakowska Av. 110/114, 02-256 Warsaw, Poland
tel.: +48 22 8460805, fax:+ 48 22 8462912
e-mail:szelag@ilot.edu.pl

Abstract

Delaminations are common defects that deteriorate strength of laminates. Delaminations can arise in the course of manufacturing due to faulty fabrication process or can result from low energy impacts, (e.g. FOD), that can take place in service. Once a delamination has been detected, a question will arise whether the defective component can still stay in service or should be immediately repaired or replaced. Before the decision is made, one of the factors that must be considered is a possible delamination growth rate under the expected service cyclic loading. One of the most effective tools that help to answer this question is a numerical simulation of delamination growth. Relatively easy way to simulate fatigue delamination growth under Mode I loading conditions is presented. The a=f(n) relationship was simulated. The simulation was performed with the help of FEM. The delamination extension resulted from gradual reduction in the stiffness of cohesive elements of length t that were located along the expected delamination path. It was assumed that the delamination would extend by Δa=t if the cohesive element stiffness dropped to 0. The applied degradation procedure of the initial mechanical properties of the cohesive elements was based on Paris low. For each delamination, extension increment the degradation process was limited to the cohesive element adjacent to the delamination front.

In case of laminates, so far, there is no standard procedure available to determine Paris low and the one used to determine it for the purpose of the simulation performed is presented, as well.

The simulation was ended when the number of cycles simulated exceeded 1000 000. The numerical results were verified against the experimental ones resulting from the four specimens tested and a satisfactory agreement was found. The difference between the a=f(n) relationship obtained by the simulation and the one being the average of the four tests was smaller than the scatter of the tests results.

Keywords: *polymeric composite, fatigue delamination, numerical simulation, fatigue test, Paris-Erdogen relationship*

1. Introduction

Delaminations can arise in the course of manufacturing due to faulty fabrication process or can result from low energy impacts, (e.g. FOD), that can take place in service. Delaminations deteriorate strength of laminates and if detected the question arises whether the defective airframe

component can still stay in service or should be immediately repaired or replaced. The decision depends on size of delamination and its growth potential under expected service loading. To answer this question numerical analysis can be helpful. At first, the delamination growth under quasi-static loading conditions should be analyzed. If the expected service static loading is low and does not produce delamination growth, i.e. the calculated strain energy release rate is lower than the critical one then the effects of expected service cyclic loading should be analyzed. Methods for analyzing delamination growth under quasi-static loading are well established, e.g. [4, 6, 8]. Numerical simulation of fatigue delamination growth is a relatively new tool that can help to assess the hazard resulting from the detected delamination. There are several ways suggested to perform it [3, 5, 7]. Nevertheless, it is a complex task especially due to the lack of needed mechanical material properties e.g. Paris-Erdogen da/dn=f(G) relationship. It should be mentioned that there is no standard method established to determine this relationship for delamination growth. Verification of numerical simulation results against experimental ones is not often presented in the accessible literature and for this reason validation of the models provided in [3, 7] is difficult .

In this paper a method for determination of Paris-Erdogen law as well as a relatively easy way to simulate fatigue delamination growth under Mode I loading conditions are presented. The numerical model was developed with the help o FEM and validated experimentally for Mode I loading. The numerically simulated a=f(n) relationship was verified against the experimental results yielded by four specimens. For this purpose carbon-epoxy, laminate, reinforced with KDU1007 UD carbon fabric, was tested in the displacement-controlled mode. ASTM E647 standard [1], which was designed for metals, was modified to determine Paris-Erdogen relationship for the laminate. This standard requires visual monitoring of crack growth, which is time consuming. To eliminate this inconvenience the new procedure was developed that took advantage of compliance changes resulting from delamination growth and allowed for delamination growth calculation.

2. Determination of Paris-Erdogen relationship

In case of laminates, so far, there is no standard procedure available to determine the Paris-Ergogen relationship needed for calculating crack growth versus number of load cycles elapsed. To some extend the method given in ASTM E647 standard could be adapted however it needs several modifications e.g. with regard to specimen design and data collection method. In the case of test, presented general requirements of ASTM E647 were fulfilled, however, several important changes had been introduced. The main steps of each procedure are schematically shown in Fig. 1. The most important changes concerned specimen geometry, Fig. 2, data collection, (Steps1, 2 and Step1 of the left and right columns, Fig. 1) and data processing, (Steps 3-5 of the left column and Steps 2-6 of the right column, Fig. 1).

A Double Cantilever Beam (DCB) specimens were used, Fig. 2. Crack growth was not visually monitored as required by ASTM E647 but consecutive crack (delaminations) lengths, $a_{i,}$ were calculated from the specimen compliance changes (1).

$$a_i = \sqrt{\frac{\delta_{i\ \max} B E_{11} h^3}{8 P_{i\ \max}}}, \tag{1}$$

where:

$\delta_{i\ max}$ – maximum relative displacement of load points in i-th cycle,
$P_{i\ max}$ – maximum load in i-th cycle,
E_{11} – Young modulus of the laminate tested, measured in the specimen longitudinal direction,
h – 1/2 of the beam, (specimen), thickness,
B – width of the beam, (specimen).

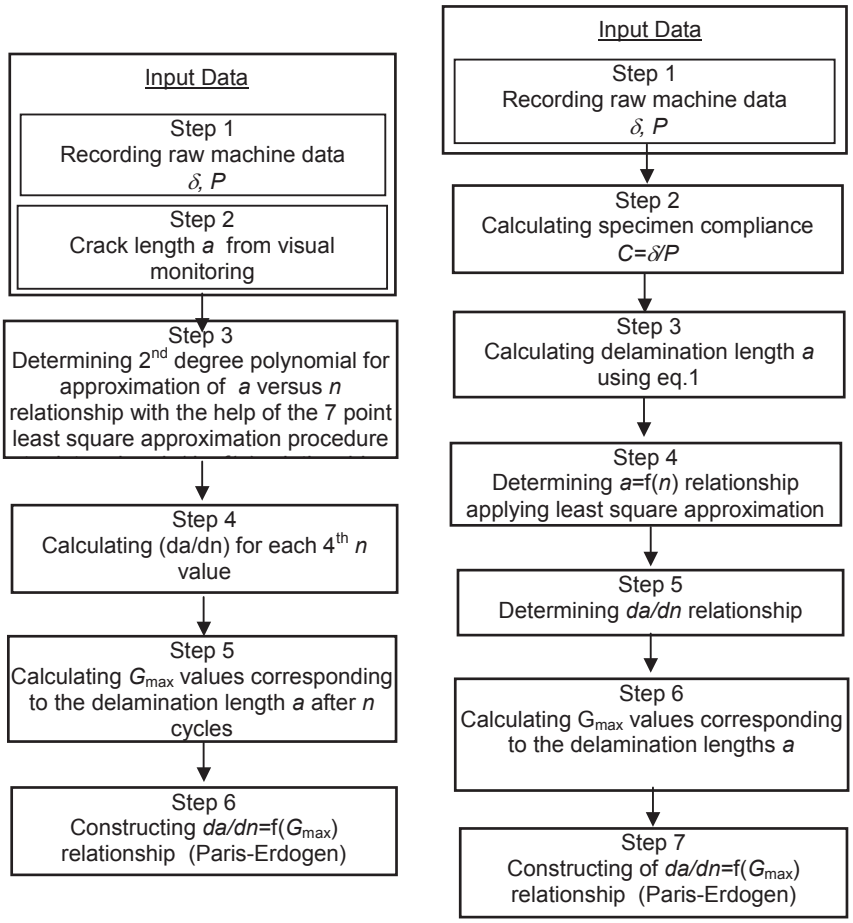

Fig. 1. ASTM E647 procedure, (left column) and proposed procedure (right column)

To calculate the specimen compliance the δ_i and P_i machine readings, (displacement of the load points and the load, respectively, see Fig.2.), were used. Because of low value of the specimen stiffness, it was assumed that the load point displacements were those of the traverse-testing machine that was used for fatigue tests.

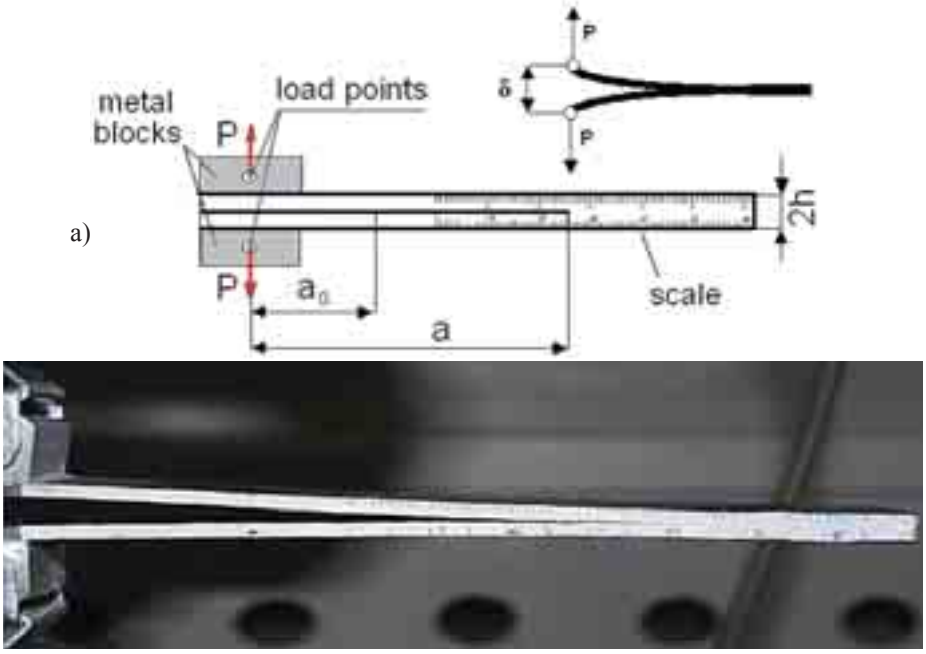

Fig.1. Double Cantilever Beam (DCB) specimens used for the determination of Paris-Erdogen law under Mode I cycling loading

2.1. Specimens and laminate tested

Wet lay-up laminate composed of 10 layers reinforced with UD carbon tape made of T300 carbon fibres was tested. The matrix was EP 53 epoxy resin cured with Z1 hardener at 60°C. Nominal fibre mass fraction was 50%. The specimens were 100 mm long and 20 mm wide with 50 mm long, crack starter placed in a middle plane of the specimen. The specimen thickness 2 h resulted from a sum of each laminate layer thickness and was equal to about 2.6mm. The opening force P was applied with the help of two metal blocks.

2.2. Test conditions

Cyclic loading of 10Hz frequency, as suggested in [2], was applied under displacement-controlled conditions. The cyclic specimen opening, δ_{max}, was chosen such that it corresponded to $G_{Imax}=0.5\ G_{IC}$ at initiation of each test. Because of displacement controlled condition $\delta_{I\,max}=\delta_{max}$ in the course of the tests. The asymmetry coefficient *R* was equal to 0.5. The tests were carried out at room temperature with the help of testing machine INSTRON ElectroPuls 3000 equipped with 3kN load cell.

2.3. Fatigue test results

An example of typical observed difference range between the crack (delamination) lengths, a_{vis}, with the use of the scale, see Fig. 1, and the calculated ones, a_{cal}, with the help of (1) is shown in Fig. 3.

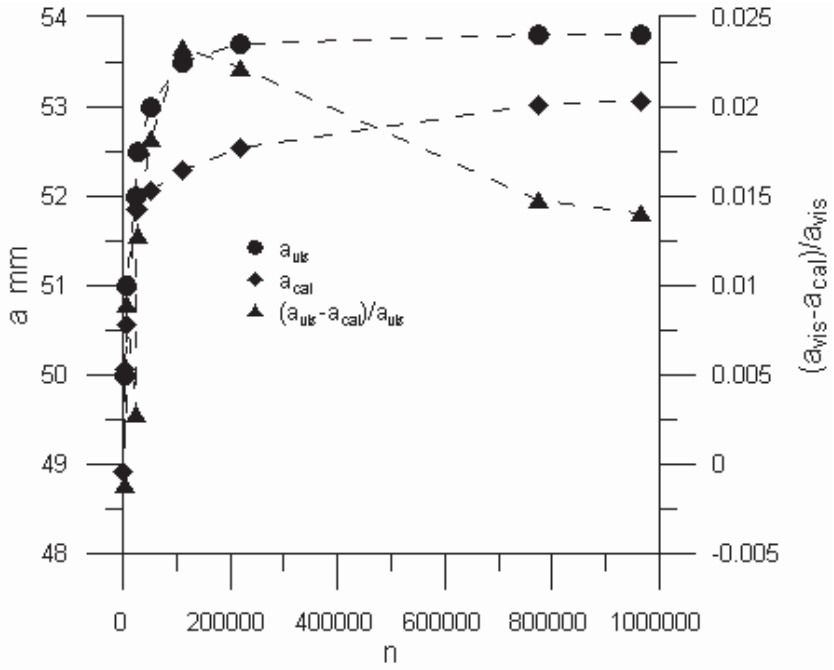

Fig. 3. Difference between the observed crack length a_{vis} and calculated crack length a_{cal} with the use of eq.1

The plot in Fig. 4 presents the Paris-Erdogen relationship (2). It was based on the results of 4 tests carried out according to the proposed modification of ASTM E647 procedure (right column in Fig. 1). Equation (2) was used for numerical simulation of the fatigue delamination growth procedure presented below.

$$\frac{da}{dn} = 10^{7.475} G_{I\max}^{17.553}. \tag{2}$$

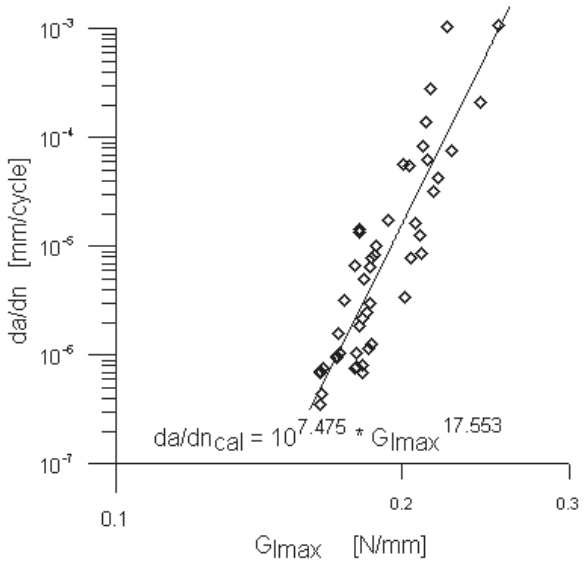

Fig. 4. Paris-Erdogen relationship obtained from 4 tests

3. Simulation of the delamination growth

The simulation was performed with the help of FEM. For this purpose, the Mentat-Marc FE code was used. The delamination extension, Δa, resulted from gradual reduction in the stiffness of cohesive elements. Cohesive elements of length t each were located along the expected delamination path i.e. the middle plane of DCB structure. It was assumed that the delamination would extend by $\Delta a=t$ if the cohesive element stiffness k_i dropped to 0. For each delamination, extension increment the degradation process was limited to the cohesive element adjacent to the delamination front. For models that can be found elsewhere [5] the fatigue degradation was not limited to one element but all the elements forming the so-called cohesive zone were involved. From the physical point of view, the latter procedure is probably more adequate but it is much more complicated from the numerical point of view. The goal of the numerical simulation presented here was a reproduction of the experimental results from the tests described in the previous section, namely a=f(n) relationship reproduction was of interest. The results obtained with the aforementioned limitation were experimentally validated. The degradation of initial mechanical properties of cohesive elements was based on the Paris-Erdogen law (2) obtained in the above-described tests. The simulation was ended when the number of cycles simulated exceeded 1000 000.

3.1. FE mode

The FE model was 2D one and it represented a laminated beam 160 mm long and 2.6 mm thick. It was initially split at the loaded end. The initial split length a_0=50mm, Fig. 1. The laminate structure was modelled with the help of 4-node orthotropic solid elements (Element 11).

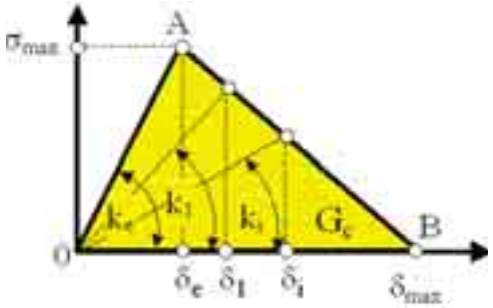

Fig. 5. Bi-linear cohesive element. There are five available parameters to define the element. They are k_e, G_c, σ_{max} δ_x and δ_{max}. However only three are independent

There were 6 elements per beam thickness used. In the middle plan of the structure, along the expected delamination path bi-linear cohesive elements were placed (Element 186). Such elements can be defined with 3 out of 5 parameters available, i.e. k_e, G_c, σ_{max} δ_e *and* δ_{max}. (depending on the FE code), Fig. 5. Application of the Mentat-Marc FE code required the definition of critical value of the Strain Energy Release Rate, (SERR), G_{Ic}, and displacements δ_e *and* δ_{max}. They were :

$$G_{Ic}=350\text{N/m},$$

$$\delta_e=0.0003\text{ mm},$$

$$\delta_{max}=0.0173\text{mm}.$$

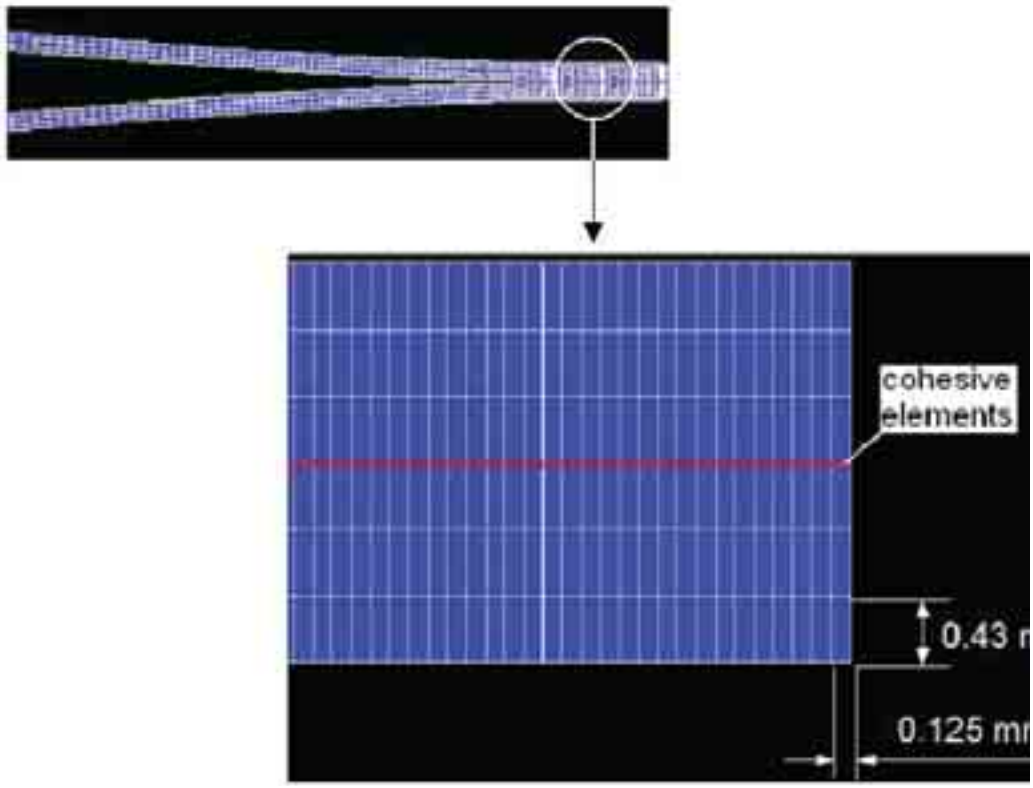

Fig. 2. Details of FE model. Red line indicates cohesive elements

Length, t, of each cohesive element was equal to 0.125mm and it was equal to the length of the solid element side each cohesive element spanned. Therefore, a failure of a single cohesive element was equivalent to an increase in the delamination length $\Delta a=t$.

3.2. Simulation procedure

The relative displacement, δ, of load points was such that condition (3) was met. The simulation was performed under displacement-controlled conditions and δ was kept constant in the course of the tests:

$$\delta_{\max} = 0.5\delta_c\,. \tag{3}$$

For each delamination length, a, the SERR value was calculated with the help of (4) (Step2):

$$G_{\max} = \frac{P\delta_{\max}}{2aB}. \tag{4}$$

Next, with the help of (2) the number of cycles needed to produce the increase in delamination length $\Delta a=t$ was calculated, (Step 4). The whole procedure had been repeated until the assumed number of cycles elapsed.

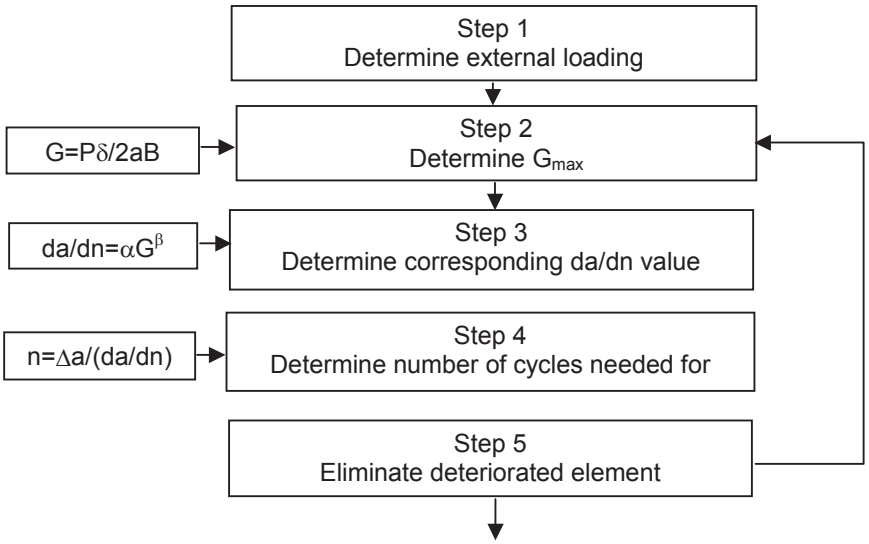

Fig. 6. Procedure for the simulation of delamination growth

3.3. Results

In Fig. 6, the numerically simulated relationship a=f(n) is represented by a continuous line. Also, for comparison, the results of four test marked with ◇❍▼▲ symbols are provided. Results of numerical simulation and those from tests were in good agreement. The maximum difference occurred for 1000000 cycles. It was in the range of 2% and was equal to about 1 mm. This value was in the range of the spread of experimental results. However, it had to be stated that the numerical simulation yielded nonconservative results since for a given number of cycles majority of experimental results were higher than those from simulation.

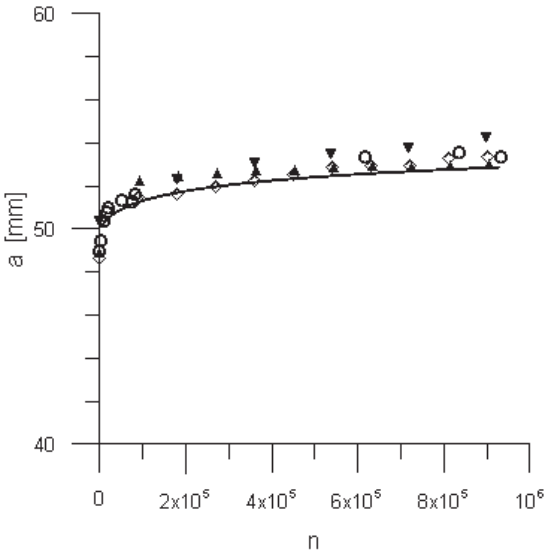

Fig. 6. Simulation versus experimental results. Continuous line represents the simulation results. Symbols ◇❍▼◢ represent results of the tests described previously

Conclusions

The carbon-epoxy laminate reinforced with KDU1007 UD carbon fabric was tested to determine the laminate resistance against Mode I delamination caused by cyclic loading. Since there is no standard procedure serving this purpose ASTM E647 standard, which is designed for testing metals, was adapted and modified. The DCB specimen geometry and loading configuration

were used. To eliminate the need for continuous visual monitoring of delamination growth during the test the delamination growth was calculated from the specimen compliance changes. To validate the procedure a comparison was made between the visual, a_{vis}, and calculated, a_{cal}, delamination lengths. The results of four tests were used to obtain the Paris–Erdogen relationship, (2). The differences were less then 3%. Such results indicated that the proposed procedure was promising. Graphs in Fig.3 show that $a_{cal.} < a_{vis}$ which was rather an unexpected result. It could be attributed to relatively long metal blocks used for loading the specimens that could make the beams stiffer. Therefore, more tests are needed to clarify the cause of this unexpected results and to make decision whether the procedure should be postponed or accepted.

Simulation of delamination growth was performed with the use of numerical model obtained with the help of FE Mentat-Marc code. The relationship a=f(n) was simulated. The results of the simulation together with the experimental ones yielded by four tests are presented in Fig. 6. The agreement was satisfactory, however, the numerical a=f(n) relationship yielded non-conservative results. It could be attributed to the way the delamination growth was mimicked. For each delamination increment, the fatigue material deterioration was limited to one cohesive element only. Such a procedure left a relatively large volume of material surrounding the delamination front not affected. The degree to which such a limitation affects the results could depend on the cohesive element size and mechanical properties of laminates. Probably a tuning of FE model could help in obtaining better results and numerical experiments serving this purpose will be carried out in the near future.

References

[1] ASTM E647-08, *Standard Test Method for Measurement of Fatigue Crack Growth Rates*.

[2] Bruner, A. J, Murphy., Pinter, G., *Development of a standarized procedure for the characterization of interlaminar delamination propagation in advanced composites under fatigue mode I loading conditions*, Engineering Fracture Mechanics, 76, pp. 2678-2889, 2009.

[3] Harper, P. W., Hallett, S. R., *A fatigue degradation law for cohesive interface elements – Development and application to composite materials*, International Journal of Fatigue, Vol. 32, I. 11, pp. 1774-1787, 2010.

[4] Riccio, A., Scaramuzzino, F., Perugini, P., *Embedded delamination growth in composite panels under compressive load*, Composites Part B32, pp. 209-218, 2001.

[5] Roe, K. L., Siegmund, T., *An irreversible cohesive zone model for interface fatigue crack growth simulation*, Engineering Fracture Mechanics, 70, pp. 209-232, 2003.

[6] Sheinman, I., Kardomateas, G. A., Pelagri, A. A., *Delamination growth during pre-and post-buckling phase of delaminated composite laminates*, Int. Journal of Solids and Structures, Vol. 35,No. 1-2, pp. 19-31, 1988.

[7] Turon, A, Costa, J., Camanho, P. P., Da´vila, C. G, *Simulation of delamination in composites under high-cycle fatigue*, Composites: Part A 38, pp. 2270–2282, 2007.

[8] Whitcomb, J. D., *Analysis of a laminate with a postbuckling embedded delamination, including contact effects*, Journal of Composite Materials, Vol. 26, No. 10, pp.1523-1535, 1992.

TESTING OF INITIATION OF ROTATING DETONATION PROCESS IN HYDROGEN-AIR MIXTURES

Włodzimierz Balicki, Andrzej Irzycki, Borys Łukasik, Krzysztof Snopkiewicz

Institute of Aviation, Propulsion Department
Krakowska Av. 110/114, 02-256 Warszawa
tel.: +48 22 8460011 ext. 337, fax: +48 8465774
e-mail: balicki@ilot.edu.pl

Abstract

The paper presents results of some research work done in the project, which aims to apply of an innovative combustion chamber to the turbine engine. Expected benefits of using of a new chamber in which classical deflagration type combustion process would be replaced with a detonation combustion type, arise from greater efficiency of Fickett-Jacobs cycle, which corresponds to rotating detonation combustion, in comparison to "classical" Brayton cycle, characteristic of deflagration combustion.

The presented task concerned fundamental research carried out on test bench designed and built at the Institute of Aviation in Warsaw. To initiate the detonation combustion in the fuel-air mixtures the ignition device of appropriately high energy is necessary. The released energy should be directed to the area where the mixture has proper constitution - preferably close to stoichiometric one.

Four different ignition manners were examined in the course of research: electrical ignition system adapted from turbine engine (semiconductor spark plug), powder charge ignition (handgun cartridges), detonation primer ignition using pentryt, and high voltage discharge (plasma jet). The appearance of detonation type combustion was identified on the basis of combustion gas pressure run, measured using piezoelectric sensors at a frequency of 1 MHz.

Keywords*: internal combustion engine, turbine engines, combustion chamber, rotating detonation*

1. Introduction

Aircraft turbine engines are a kind of “transducers”, in which the chemical energy contained in fuel is converted into thrust. This “treatment” is bound to incurring engine's manufacturing and operating cost (including fuel costs, repairs), and the costs of charging of the environment in which we live with noise and toxic exhaust gas components. Current trends in development of these engines are driving towards increasing of service life (e.g. one of CF6-80C2 aircraft motors operated on the Boeing 767 at LOT attained overhauling period of 27,000 hours) as well as reducing fuel consumption through increase efficiency and reduction of nitrogen oxides and unburned hydrocarbons and soot content in the exhaust. The chance of realizing of above-mentioned goals gives modification of combustion process which proceeds in engine’s combustion chambers, namely replacement of classical combustion with detonative-deflagration type combustion (see Tab. 1).

Tab. 1. Differences between deflagration and detonation processes [5, 6]

Feature	Deflagration	Detonation
Flame front velocity	Combustion velocity of the order of dozen m/s	Detonation velocity of the order of km/s
Dimensions of combustion chamber	Large combustion chamber	Short combustion zone
Composition of fuel mixture	Combustion at stoichiometric ratio	Combustion (detonation) of lean mixture
Exhaust gas temperature	Very high temperature	Lower temperature
Emission of nitrogen oxides	High emission of NOx	Low NOx emission
Need for cooling exhaust gas at the outlet from the chamber	Necessity to mix extra air before turbine	No necessity to mix extra air
Change of gas pressure in the chamber	Pressure drop due to combustion	Pressure increase due to detonation
Construction simple / complex		More simple design